ELSEVIER

Agricultural and Forest Meteorology 2915 (2000) 1–27

AGRICULTURAL AND FOREST METEOROLOGY

www.elsevier.com/locate/agrformet

A spectral analysis of biosphere–atmosphere trace gas flux densities and meteorological variables across hour to multi-year time scales

Dennis Baldocchi [a,*], Eva Falge [a,b], Kell Wilson [c]

[a] *Department of Environmental Science, Ecosystem Science Division, Policy and Management, 151 Hilgard Hall, University of California, Berkeley, CA 94720-3110, USA*

[b] *Plant Ecology, University of Bayreuth, 95440 Bayreuth, Germany*

[c] *Atmospheric Turbulence and Diffusion Division, NOAA, PO Box 2456, Oak Ridge, TN 37831, USA*

Received 7 February 2000; received in revised form 13 September 2000; accepted 29 September 2000

Abstract

The advent of long-term studies on CO_2 and water vapor exchange provides us with new information on how the atmosphere and biosphere interact. Conventional time series analysis suggests that temporal fluctuations of weather variables and mass and energy flux densities occur on numerous time scales. The time scales of variance that are associated with annual time series of meteorological variables, scalar flux densities and their covariance with one another, however, remain unquantified.

We applied Fourier analysis to time series (4 years in duration) of photon flux density, air temperature, wind speed, pressure and the flux densities of CO_2 and water vapor. At the daily time scale, strong spectral peaks occurred in the meteorological and flux density records at periods of 12 and 24 h, due to the daily rising and setting of the sun. At the synoptic time scale (3–7 days) the periodic passage of weather fronts alter available sunlight and temperature. In turn, variations in these state variables affect carbon assimilation, respiration and transpiration. At the seasonal and semi-annual time scales, a broad spectral peak occurs due to seasonal changes in weather and plant functionality and phenology. In general, 21% of the variance of CO_2 exchange is associated with the annual cycle, 43% of the variance is associated with the diurnal cycle and 9% is associated with the semi-annual time scale. A pronounced spectral gap was associated with periods 3–4 weeks long.

Interactions between CO_2 flux density (F_c) and sunlight, air temperature and latent heat flux density were quantified using co-spectral, coherence and phase angle analyzes. Coherent and in-phase spectral peaks occur between CO_2 exchange rates and water vapor exchange on annual, seasonal and daily time scales. A 180° phase shift occurs between F_c and photon flux density (Q_p) on seasonal and daily time scales because the temporal course of sunlight corresponds with the withdrawal of CO_2 from the atmosphere, a flux that possesses a negative sign. Covariations between F_c and T_{air} experience a 180° phase shift with one another at the seasonal time scale because rising temperatures are associated with more carbon uptake. At daily time scales the phase angle between F_c and T_{air} is on the order of 130°. This phase lag can be explained by the strong dependence of canopy photosynthesis on available light and the 2–3 h lags, which occur between the daily course of sunlight and air temperature.

*Corresponding author. Tel.: +1-510-643-5098; fax: +1-510-642-2874.
E-mail address: baldocchi@nature.berkeley.edu (D. Baldocchi).

PII: S0168-1923(00)00228-8

Spectral analysis was used to investigate the performance of a biophysical model (CANOAK) across a spectrum of time scales. By varying meteorology, leaf area index and photosynthetic capacity, the model was able to replicate most of the spectral gaps and peaks that were associated with CO_2 exchange, when soil moisture was ample.

Keywords: Fourier analysis; Evaporation; Carbon dioxide exchange; Micrometeorology; Biometeorology; Energy exchange; Biosphere–atmosphere interactions

1. Introduction

The natural environment constantly experiences temporal variation. The daily and seasonal march of the sun across the sky, the passage of clouds across the sun's face, gusts of wind and the seasonal changes in plant structure and function are common, every day examples of factors that induce such variation.

The topic of this paper is on the temporal variation of CO_2 and water vapor flux densities between a temperate deciduous forest and the atmosphere. Relevant time scales of temporal variation in meteorological forcing variables, such as wind, temperature and sunlight, and coupled biological processes, such as photosynthesis, respiration and evaporation, range from fraction of seconds to years (Kaimal et al., 1972; Anderson et al., 1986; Jarvis, 1995; Pielke et al., 1998; Baldocchi and Wilson, 2000). The dynamic response of ecosystem CO_2 and water vapor exchange to an environmental perturbation depends on the combined response of the ecosystem's component compartments. Ecosystem CO_2 exchange, e.g. is comprised of assimilation from one compartment (leaves) and respiration from four compartments (leaves, boles, roots and soil organic matter). Canopy evaporation, on the other hand, consists of water vapor that is lost through plant transpiration, soil evaporation and the evaporation of free water that may exist on leaves after dew or rain. How fast each compartment responds to an environmental perturbation depends upon its size and its time constant (Schimel et al., 1996; Braswell et al., 1997; Randerson et al., 1999).

Short-term (less than 1 h) variations in canopy CO_2 exchange are forced by changes in photosynthesis, stomatal conductance, and respiration. In general, photosynthesis and stomatal conductance respond differently to slow and fast changes in sunlight. Depending on their state of induction, it can take seconds to tens of minutes for photosynthesis and stomatal conductance to reach a new equilibrium after a change in sunlight (Pearcy, 1990), as when a cloud passes the sun. Changes in sunlight also affect a leaf's temperature and transpiration rate. Such changes are important because concomitant changes in temperature alter rates of leaf respiration (Jones, 1983; Su et al., 1996). The finite heat capacity of leaves and mutual shading, however, buffer changes in temperature that are imposed by changes in the radiation balance (Jones, 1983; Su et al., 1996). So leaf respiration will not change as quickly to changes in sunlight as will photochemical reactions linked to the electron transport cycle of photosynthesis. On the other hand, the thermal capacity of leaves is much less than that experienced by the soil, so temperature-dependent leaf processes will experience more variability than will temperature-dependent processes in the soil.

On the diurnal time scale (24 h), variations in CO_2 and water vapor exchange are forced by daily rhythms in solar radiation, air and soil temperature, humidity, and CO_2 (e.g. Jarvis et al., 1997; Baldocchi, 1997). Notable impulses occur near sunrise and sunset, as the biosphere changes from gaining carbon and losing water during the day to losing carbon at night.

Weekly fluctuations in CO_2 and water exchange can be induced from synoptic weather changes that are associated with the passage of high and low pressure systems and fronts. These events will cause distinct periods of clear skies, overcast, and partly cloudy conditions. The passage of weather events alter the amount of light available to an ecosystem and they affect how light is transmitted through a plant canopy and how it is used to assimilate carbon. For instance, canopy photosynthesis is more efficient under cloudy skies (Jarvis et al., 1985; Hollinger et al., 1994; Ruimy et al., 1995; Baldocchi, 1997; Gu et al., 2000). The passing of weather fronts also changes air temperature, humidity deficits, and pressure. Weather fronts, therefore, can impose weekly scale fluctuations on photo-

synthesis, respiration and stomatal opening, as these physiological processes respond to changes in cited meteorological variables.

Often overlooked, at weekly time scales, is the role of pressure and precipitation on CO_2 efflux from the soil. Changes in pressure or fronts of water in the soil by rain will restrict or enhance the transfer of CO_2 gases from the soil (carbon dioxide: Kimball, 1983; radon: Clements and Wilkening, 1974).

The frequency of precipitation can re-enforce itself through the occurrence of persistent drought and wet spells (Brubaker and Entekhabi, 1996; Fennessy and Shukla, 1999). Dry spells can exert a significant reduction on the net ecosystem CO_2 and water vapor exchange, as compared to periods when soil moisture is ample (Baldocchi, 1997), by restricting photosynthesis and respiration.

Frontal passages may also cause the measurement of ecosystem CO_2 exchange, by the eddy covariance method, to be biased. Associated changes in wind direction and speed may cause a tower site to view a different flux footprint (Amiro, 1998). The implication of this effect is to view different patches of underlying vegetation, which may have different functionality and capacity for trace gas exchange.

On monthly to seasonal times scales, an ecosystem starts to experience the effects of the seasonal change in the sun's position, which includes the potential amount of sunlight received, surface temperature and the soil water balance. Superimposed upon slow variations of these meteorological factors is variation attributed to an ecosystem's phenology. Examples include the timing and occurrence of leaf expansion and growth, seasonal changes in photosynthetic capacity, leaf area index, and leaf-fall (Wilson et al., 2000). The timing of leaf-out, for instance, has a distinct impact on the humidity and temperature of the planetary boundary layer (Schwartz, 1996) and the Bowen ratio at the Earth's surface (Wilson and Baldocchi, 2000).

At inter-annual time scales, the timing of phenological switching events, such as leaf-out, may be advanced or delayed by a month due to large-scale climatic features that can be associated with *El Nino–La Nina* cycles (Myneni et al., 1997; Keeling et al., 1996). Growing season duration has a profound influence on net biosphere productivity (Lieth, 1975; Baldocchi and Wilson, 2000) and can have a major impact on inter-annual fluxes of carbon dioxide (Randerson et al., 1999).

In order to study the spectrum of times scales we have identified, one needs multi-year and quasi-continuous records of mass and energy fluxes, and associated meteorological variables. As recent as a few years ago, such information was not available. But this condition is being ameliorated through the auspices of the AmeriFlux, Euroflux and FLUXNET projects (Running et al., 1999; Valentini et al., 2000) and the efforts of scientists working on those projects. Several research teams started making CO_2 and water vapor flux measurements in the early 1990 s (e.g. Wofsy et al., 1993; Black et al., 1996; Greco and Baldocchi, 1996; Valentini et al., 1996; Goulden et al., 1997), and now have over 5 years of data.

So far, most investigators studying trace gas fluxes between the biosphere and atmosphere have treated their data with now familiar plots of times series. Or investigators have inferred temporal dynamics of biosphere–atmosphere CO_2 exchange, indirectly, by examining long-term records of CO_2 concentration (e.g. Braswell et al., 1997; Randerson et al., 1999).

The interplay between trace gas exchange processes and their environmental drivers can introduce phase lags, filtering, amplifications and chaos on signals being assessed (Hamming, 1989; Zeng et al., 1990; Turchin and Taylor, 1992; Schimel et al., 1996; Braswell et al., 1997). Spectral analysis is a quantitative tool that can be used to evaluate complex temporal patterns that may be exhibited in long time series. Fourier analysis, in particular, transforms a stochastic time series into a sum of periodic sine waves. Fourier analysis is thereby able to quantify the amount of variance (or power) that is associated with a particular frequencies or periods. The method has been used numerous times to examine spectral features of atmospheric turbulence (e.g. Kaimal et al., 1972; Kimball, 1983; Anderson et al., 1986) and climate records (Heusser et al., 1999; Ridgewell et al., 1999). The application of spectral analysis to intermediate-length meteorological records, on the other hand, is rare (Van der Hoven, 1957; Heggem et al., 1998; Wikle et al., 1999). And no investigator, to our knowledge, has applied spectral analysis to investigate the relative

variance that is associated with multiplicity of time scales are observed upon the annual record of meteorological variables and direct measurements of biogeochemical flux densities, such as CO_2 and water vapor.

We advocate use of spectral analysis to draw new insights on patterns of trace gas fluxes and their meteorological forcing over multiple time scales. Spectral analysis can be used to quantify how much power is associated with well-known periodicities such as the daily and annual cycles. It can also be used to quantify the impact of variance generated by fronts, early or late springs, summer droughts or wet cloudy years. The analysis of covariance, coherence and phase lags can be used to interpret how environmental variables force whole canopy CO_2 and water vapor exchange across various time scales.

We have been measuring carbon, water and energy exchange on a nearly continuous basis over a temperate forest since October 1994. From these measurements we constructed continuous year-long data sets for the years 1995 through 1998 and have applied Fourier analysis to evaluate the spectral properties of these data records. The first objective of this paper is to examine the properties of the power spectra of meteorological variables and flux densities of CO_2, water vapor and sensible heat over a broad-leaved deciduous forest. We aim to identify periodicities and the relative variance associated with diurnal swings, passage of fronts, seasonal effects such as drought, leaf-out and leaf-fall. The second objective of this work is to investigate how environmental factors interact with canopy photosynthesis, respiration, evaporation and the generation of sensible heat. To attain this means, we examine co-spectra, coherence and phase lags between relevant trace gas flux densities and governing meteorological variables, such as sunlight and temperature. Our third and final objective is to combine our data analysis with model calculations to examine how well a biophysical trace gas exchange model (CANOAK; Baldocchi, 1997) simulates the spectrum of frequencies that comprise an annual sum of CO_2 exchange. This last exercise provides insight on how well we are representing seasonal trends in model parameters such as photosynthetic capacity and leaf area index.

2. Materials and methods

2.1. Site characteristics

The experimental field site is located on the United States Department of Energy reservation near Oak Ridge, TN (latitude 35°57′30″N; longitude 84°17′15″W; 335 m above mean sea level). Vegetation at the site consists of mixed-species, broad-leaved forest, growing in the eastern North American deciduous forest biome. The predominant species in the forest stand are oak (*Quercus alba* L., *Q. prinus* L.), hickory (*Carya ovata* (Mill.) K. Koch), maple (*Acer rubrum* L.), tulip poplar (*Liriodendron tulipifera* L.) and loblolly pine (*Pinus taeda* L.). The forest has been growing since agricultural abandonment in 1940. The mean canopy height was about 26 m. The peak leaf area index of the canopy typically occurs by day 140 and reaches about 6.0. The soil is classified as a Fullerton series, Typic Paleudult, otherwise described as an infertile cherty silt-loam. A thorough description of the site is presented in Hutchison and Baldocchi (1989).

2.2. Measurements, instrumentation and calculations

The eddy covariance method was used to measure trace gas flux densities between the biosphere and atmosphere. A set of micrometeorological instruments was supported 36.9 m above the ground (10 m over the forest) on a 44 m tall walk-up scaffold tower. The tower is located on a spur ridge. Wind velocity and virtual temperature fluctuations were measured with a three-dimensional sonic anemometer (Applied Technology, Boulder, CO). Carbon dioxide and water vapor fluctuations were measured with an open-path, infrared absorption gas analyzer (Auble and Meyers, 1992). The fast response CO_2/water vapor sensor was calibrated against gas standards. The calibration standards for CO_2 were traceable to those prepared by NOAA's Climate Monitoring and Diagnostic Laboratory. The output of the water vapor channel was referenced to a dew point hygrometer. Corrections for density fluctuations on CO_2 and water vapor flux covariances, as measured with the open path sensor, were applied (Webb et al., 1980; Paw U et al., in press).

Micrometeorological data were sampled and digitized 10 times per second. In-house software was used

to process the measurements. The software computed covariances between velocity and scalar fluctuations over half-hour intervals. Turbulent fluctuations were calculated from the difference between instantaneous and mean quantities. Mean velocity and scalar values were determined, in real-time, using a digital recursive filter. The digital filter algorithm employed a 400 s time constant.

The CO_2 storage term was estimated, by finite difference, with a CO_2 profile measurement system. An automatically controlled, solenoid sampling system directed air into an infrared gas analyzer (model LI 6262, LiCor, Inc., Lincoln, NE). Air was sampled from four levels above and within the forest (36, 18, 10, 0.75 m). Air from each level flowed through the analyzer for 30 s and data were sampled during the last 20 s of sampling. This scheme allowed a direct measurement of the profile every 120 s. The gas measurement system was automatically calibrated each day at midnight by passing gases of known concentration through the analyzer.

2.3. Computational methods and data

We evaluated the time series of meteorological variables and flux densities of CO_2, water vapor and sensible heat flux using Fourier analysis (Panofsky and Dutton, 1984; Bracewell, 1990). Specifically, fast Fourier method (Carter and Ferrier, 1979; Press et al., 1992) was used to compute power spectra, co-spectra and phase angle spectra. The power spectrum provides information on how much variance is associated with particular frequencies. The co-spectrum quantifies the amount of covariance that occurs between to variables, x and y, across a spectrum of frequencies. Coherence and phase angle spectra give information on the relation between the co-spectrum (Co_{xy}) and quadrature (Q_{xy}) spectrum. Coherence is defined as

$$\mathrm{Coh}(n) = \frac{\mathrm{Co}_{xy}(n)^2 + Q_{xy}(n)^2}{S_{xx}(n)S_{yy}(n)} \quad (1)$$

and phase angle is

$$\phi_{xy}(n) = \tan^{-1}\left(\frac{Q_{xy}(n)}{\mathrm{Co}_{xy}(n)}\right) \quad (2)$$

In these equations, n represents natural frequency.

The numerical scheme we used, applies the fast Fourier technique to time series that contain a number of samples that is a power of 2. We computed two mean samples per hour, so over the course of a year there were 17,520 half-hour periods. The number, 16,384 (2^{14}), is the closest power-of-two multiple to this value. It represents 93% of a year, so the lowest frequency we can resolve with a fast Fourier transform is $0.000122\,\mathrm{h}^{-1}$. The highest frequency we are able to resolve in this analysis is one cycle per hour, as defined by the Nyquist frequency.

When applying the fast Fourier transform to the data, the mean was removed from the original time series to reduce red noise. A cosine window was applied to the time series to eliminate the Gibbs phenomenon (spectral 'ringing') that is associated with truncated and discrete time series (Hamming, 1989). Spectral coefficients were smoothed and block-averaged to reduce scatter and to suppress aliasing by higher frequency components (Kaimal and Finnigan, 1994). We contend that the effect of aliasing, on computing spectra, is negligible because the original time series of flux data were sampled at 10 Hz and the meteorological data were sampled at 1 Hz.

The data evaluated in this paper were acquired during 1995–1998. It is impossible to measure trace gas fluxes during every period of the year because of occasional problems associated with instrumentation and the interpretation of micrometeorological fluxes. Consequently, we used gap-filling methods to replace missing or bad data as recommended by Press et al. (1992). With regards to the mass and energy fluxes we used a method based on "look-up"-tables (Falge et al., 2000); we eschewed the use of regressions models for gap-filling, as they constrained the shape of the functional relationship between the dependent and independent variables, which can lead to bias errors. For CO_2 exchange, "look-up" tables were generated by sorting flux densities according to quantum flux density (Q_p) and air temperature (T_a). For latent heat flux density, quantum flux density (Q_p) and vapor pressure deficit (D) were chosen as sorting variables for the "look-up" table (see Verma et al., 1986). The respective variables were sorted by 2°C temperature intervals, 0.15 kPa vapor pressure deficit intervals or $100\,\mu\mathrm{mol\,m^{-2}\,s^{-1}}$ intervals for Q_p.

"Look-up" tables were created for 2-month periods that were demarked by distinct phenoseasons. Unique

Table 1
Statistics on the percentage of gaps that are associated with the time series of net CO_2 and latent heat flux densities

Year	NEE, gap percentage			LE, gap percentage		
	Day	Total	Night	Day	Total	Night
1995	33.9	41.5	49.1	26.5	30.5	34.6
1996	35.3	42.8	50.5	23.8	27.4	31.0
1997	39.7	47.7	55.8	26.5	30.1	33.8
1998	52.7	56.8	61.0	31.1	32.9	34.7

look-up tables were created for the spring transition (days 90–151), the summer growing season (days 152–273), autumnal senescence (days 274–334) and the winter dormant period (days 335 through 89). A summary of the gap-filling record is listed in Table 1. We do not expect gap-filling to introduce significant biases to our spectral analysis as the gaps were random and the summation of net ecosystem CO_2 exchange was independent of gap size, as long as gaps were less than 40% of the total annual record (Falge et al., 2000).

Gaps in meteorological data were filled in different manner. We computed mean diurnal patterns by binning data according by hour. Missing data were filled with the corresponding quantity. The mean diurnal course was updated over the season with a running mean. Overall, the number of gaps in the meteorological record was small, on the order of 1–2%.

3. Results and discussion

3.1. Climate

In order to understand the climatic forcing on the atmosphere and biosphere, we first provide information on climate conditions encountered during the experiment period (Table 2); a full discussion on these issues is provided in Wilson and Baldocchi (2000).

Over the 4-year study period, the annual sums of precipitation ranged between 1400 mm (1995) and 1693 mm (1998). For reference, the 30-year average annual precipitation near the site is 1372 mm. In 1995, annual precipitation was only about 10% below normal. But, 1995 is considered to be a drought year as the total precipitation during the critical 3-month summer growing period of June–August 1995 was particularly low (165 mm compared to the average

Table 2
Climate summary of atmospheric state variables, energy balance components and bulk canopy characteristics over the duration of the field experiment

Variable	1995	1996	1997	1998
Solar radiation ($GJ\,m^{-2}$)	5.45	5.43	5.41	5.21
Mean temperature (°C)	15.3	14.5	14.9	16.5
Precipitation (mm)	1400	1690	1659	1693
Maximum leaf area index	NA	5.5	6.0	6.3
Net radiation R_n ($GJ\,m^{-2}$)	3.17	2.93	3.01	2.80
Latent energy flux LE ($GJ\,m^{-2}$)	1.31	1.36	1.50	1.48
Sensible heat flux H ($GJ\,m^{-2}$)	1.11	0.97	1.08	1.11
Spring (day CO_2 flux changes sign)	105	121	108	106
Autumn (day CO_2 flux changes sign)	305	315	314	325
Estimated growing season length (days)	200	194	206	219
Maximum leaf nitrogen ($mg\,g^{-1}$)	NA	23.0	21.0	NA

343 mm for these 3 months; Baldocchi, 1997). In contrast, precipitation during the summer growing season was above average during 1996 (413 mm), 1997 (558 mm) and 1998 (400 mm).

The 30-year normal temperature is 13.9°C at a nearby climate-monitoring station (Oak Ridge, TN). The annual departures from the mean were +1.4°C (1995), +0.6°C (1996), +1.0°C (1997) and +2.6 (1998). During the 3-month summer growing period of June–August, the departures from normal were +2.4°C (1995), +1.6°C (1996), +1.0°C (1997) and +2.43 (1998). The 1998 study year was especially noteworthy as it was an 'El Nino' year, which in the southeastern United States was a year that was warmer and wetter than normal.

Continuous measurements of leaf area were estimated using light transmission measurements. These estimates were calibrated each year with independent leaf litter-fall measurements. Maximum values of leaf area were on the order of 5.5–6.0. The seasonal dynamics of leaf area and its inter-annual variability, over the 4-year interval, is shown in Fig. 1. The emergence of leaves, in spring, began before day 100 during 1995, 1997 and 1998. Leaf development was delayed by about 2 weeks in 1996, as compared to this cohort of years. Cool cloudy periods in 1997 and 1998 delayed the date of full leaf expansion to nearly that observed in 1996, which occurred between days 130 and 140. In contrast, the canopy achieved full-leaf by day 118 during 1995.

Like spring leaf-out, the dates of senescence and complete leaf fall varied among the 4 years. The year

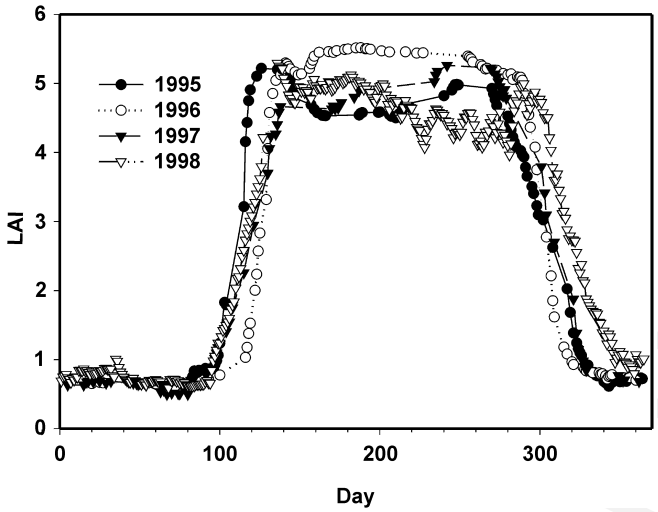

Fig. 1. The seasonal variation of leaf area index of a temperate deciduous forest measured during 1995–1998. The data were inferred using light transmission measurements and Beer's law. The inferential estimates of leaf area index were calibrated using litter collection baskets.

with earliest senescence was 1995. Leaf area started to diminish around day 280 and the canopy was bare by day 320. The year with the latest senescence was 1998. Leaf area index did not start to decrease until day 300 and leaves were present on the trees until day 345.

The lengths of the physiologically active season were estimated from the approximate dates when the daily flux of carbon dioxide crossed the zero point on the *y*-axis in spring and again in autumn (Table 2). These data show that the duration of net carbon uptake and transpiration ranged from 194 to 219 days.

3.2. Power spectra of plant and meteorological variables

In order to understand the power spectra of CO_2 and water vapor exchange, over the course of a year, it is essential to examine the power spectra of important plant and environmental forcing variables first.

The square-wave shape of the seasonal time course of leaf area index, during a representative year, 1996, produces a power spectrum that peaks with a period of 205 days (0.00487 per day) (Fig. 2). A steep spectral drop-off occurs for periods equal to 68 days (0.0147 per day). The representation of a non-sinusoidal wave as the summation of sinusoidal waves produces spectral peaks at frequencies higher than that of the spectral gap (0.0144 per day).

Figs. 3–6 show the power spectra for quantum flux density of photosynthetically active radiation (Q_p), air temperature (T_a), wind speed (u) and atmospheric pressure (P), respectively, for the time series acquired from 1995 through 1998. The power spectral densities are multiplied by natural frequency (n) and are normalized by their respective variances. This normalization scheme, when plotted on a log–log scale, yields unity when integrated from zero to infinity.

The power spectra for ecologically important, meteorological variables show both common and distinct features involving the position of spectral peaks and gaps. Regarding common features, the power spectra for visible sunlight (Q_p) and air temperature (Figs. 3 and 4, respectively) show distinct spectral peaks at high and low frequencies. The high frequency peaks have periodicities (inverse frequency) of 12 h (0.00347 h^{-1}) and 24 h (0.00174 h^{-1}). The low frequency peak is broad and spans periods with seasonal to semi-annual (3–6 month) time scales (0.0002–0.0004 h^{-1}).

The daily switch between day and night and the daily revolution of Earth are responsible for the higher frequency peaks in the sunlight and air temperature

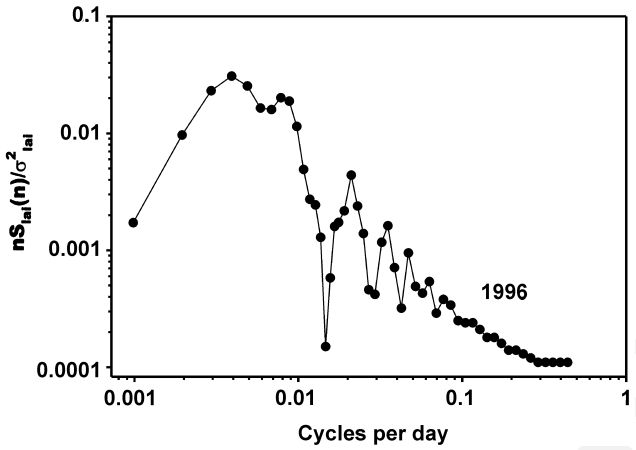

Fig. 2. The power spectrum of leaf area index measured during 1996. The spectral densities are multiplied by natural frequency, n, and are normalized by the variance of the time series.

power spectra. The spectral peak on the seasonal to semi-annual time scales is a feature of the seasonality of distinct differences in climate during winter, spring, summer and autumn and the half-year duration of the growing season. One would expect this peak to differ over tropical, agricultural, boreal and Mediterranean systems, where growing season lengths differ or are shifted in phase.

Midrange between the seasonal and daily spectral peaks is a pronounced spectral gap. In general, it is associated with the monthly time scale, but its periodicity is imprecise and ranges between 20 and 40 days (0.00208–0.00104 h^{-1}), over the course of the 4-year study. These results refute any pre-supposition that these meteorological variables may be forced by the lunar cycle, as are ocean tides.

Regarding dissimilarities in the low ($n < 0.0003\,h^{-1}$) frequency region of the sunlight and temperature power spectra, we observe that the seasonal peak is much less pronounced (by a factor of 10) for Q_p than for air temperature (T_a). At the high frequency band of the power spectrum ($n > 0.10\,h^{-1}$), the normalized power spectrum of visible sunlight, Q_p, is flat. This feature does not suggest white noise, however. With our normalization scheme, $a + 1$ slope characterizes white noise. Instead it means that variance is distributed evenly across the range of frequencies. The random nature of cloud fields is one contributor to this observation. The temperature power spectra, in contrast, exhibit a 'spectral-cascade' in the frequency domain between 0.005 and 1 cycles h^{-1} (except for distinct peaks with 12 and 24 h periodicities). The slopes of the spectral drop-off at the high frequency end (n ranging from 0.5 to 1 h^{-1}) of the temperature power spectrum were −0.96, −0.70, −1.32 and −1.51, respectively, for the years 1995 through 1998. For comparison, the spectral slope that occurs in the inertial sub-range of a turbulence spectrum equals $-\frac{2}{3}$ at periods shorter than 1 h (Anderson et al., 1986).

The power spectrum for wind speed (Fig. 5) possesses many contrasts, as compared to the sunlight and temperature spectra. For instance, the wind speed spectrum does not show a spectral peak with a 12 h periodicity (except during 1996). More notably, we do not observe a spectral gap in the 1–3 h period range of the wind speed spectrum, as has been suggested by Van der Hoven (1957) and some meteorological textbooks (Panofsky and Dutton, 1984). Those pioneering results, however, have not been substantiated with modern and extended measurements, using aircraft (Wikle et al., 1999) and towers (Heggem et al., 1998). Modern wind measurements indicate that an inertial subrange for wind extends from wavelengths of 1 to 1000 km (Wikle et al., 1999).

The slope of the wind speed spectrum in the region of the spectral cascade is about −0.24 (or −1.24 when plotted as a function of $S_u(n)$). The measured slopes of power spectra for long wavelengths do not conform to

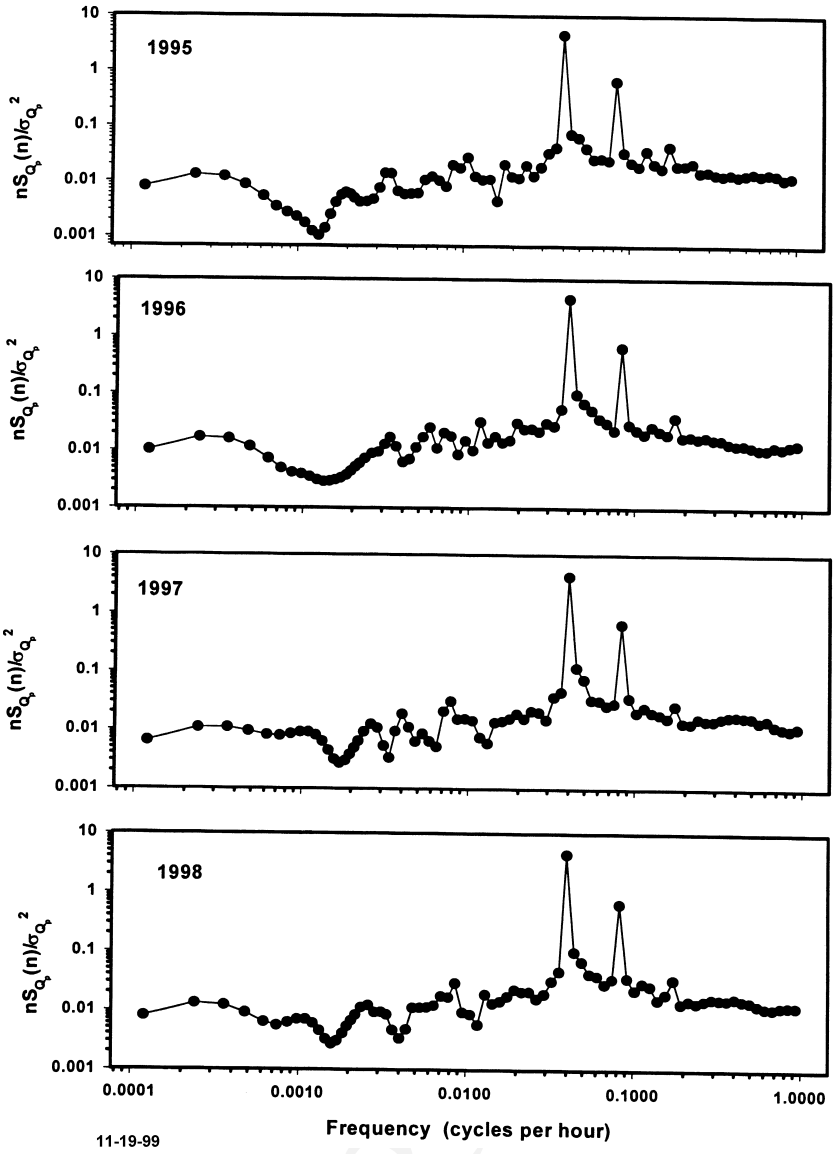

Fig. 3. Power spectrum for a year-long time series on photosynthetically active radiation flux density (Q_p). The spectral densities are multiplied by natural frequency, n, and are normalized by the variance of the time series. Spectra are presented for the years 1995 (a), 1996 (b), 1997 (c), and 1998 (d).

standard turbulence theory provided by Kolmogorov scaling ($S(\kappa) = \alpha\varepsilon^{2/3}\kappa^{-5/3}$; $\kappa S(\kappa) = \alpha\varepsilon^{2/3}\kappa^{-2/3}$, where α is the Kolmogorov constant, k the wavenumber and ε is the turbulence dissipation rate). In contrast, Wikle et al. (1999) report that the wavenumber slope of the inertial subrange for wind spectra measured over the ocean is about $-\frac{5}{3}$ for wavelengths ($\lambda = 1/\kappa$) between 1 and 1000 km, though they cite studies with slopes up to -2.5. The reader should view the slopes of our time-based wind speed and temperature spectra with caution, as we must rely on Taylors' frozen eddy hypothesis to convert frequency to wavenum-

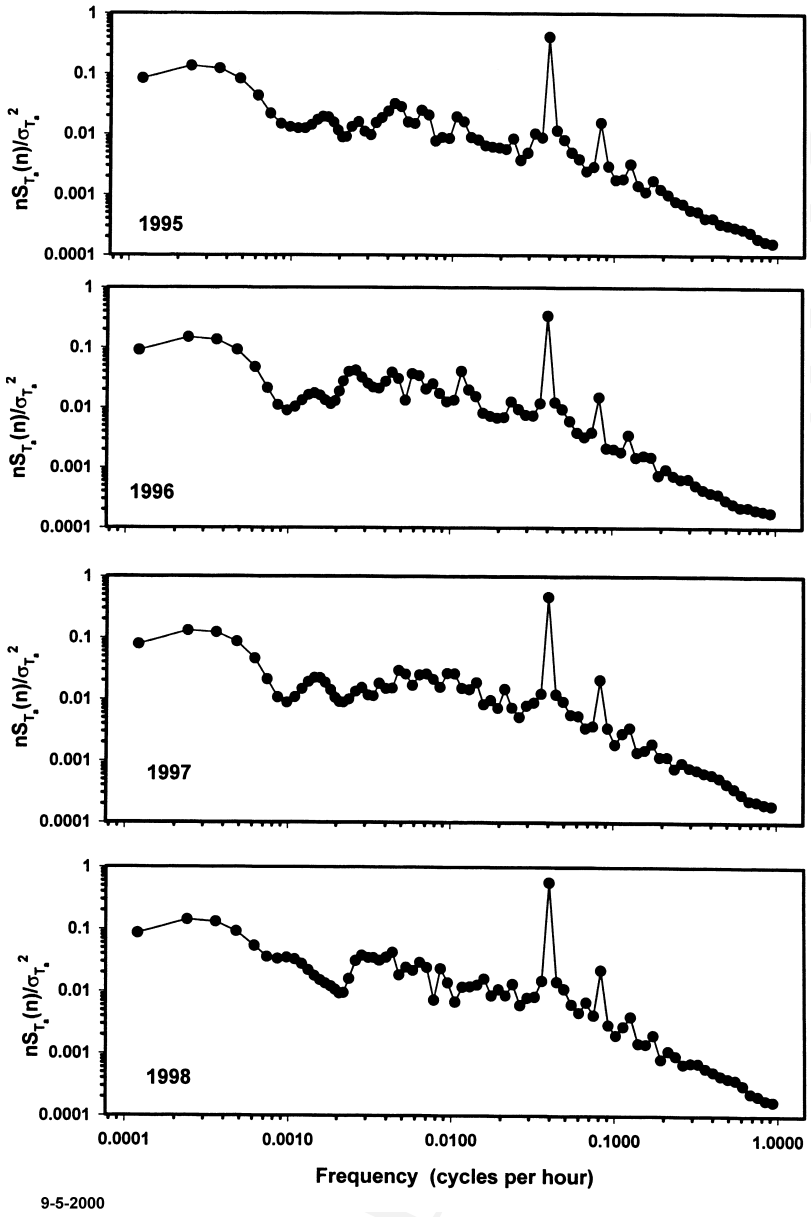

Fig. 4. Power spectrum for a year-long time series on air temperature (T_a). The spectral densities are multiplied by natural frequency, n, and are normalized by the variance of the time series. Spectra are presented for the years 1995 (a), 1996 (b), 1997 (c), and 1998 (d).

ber ($\kappa = f/u\,\mathrm{m}^{-1}$) (see Panofsky and Dutton, 1984). Strong wind shear (which is observed at night during stable thermal stratification) and non-stationarity cause Taylor's frozen eddy hypothesis to be invalid (Panofsky and Dutton, 1984). In contrast, Wikle et al. (1999) derived their data using aircraft transects over the tropical Pacific Ocean. They did not need to invoke Taylor's frozen eddy hypothesis since they were able to measure wavenumbers directly.

Fig. 6 presents a power spectrum for atmospheric pressure. These data are presented with the intent to identify if any periodicities are imposed on CO_2 and

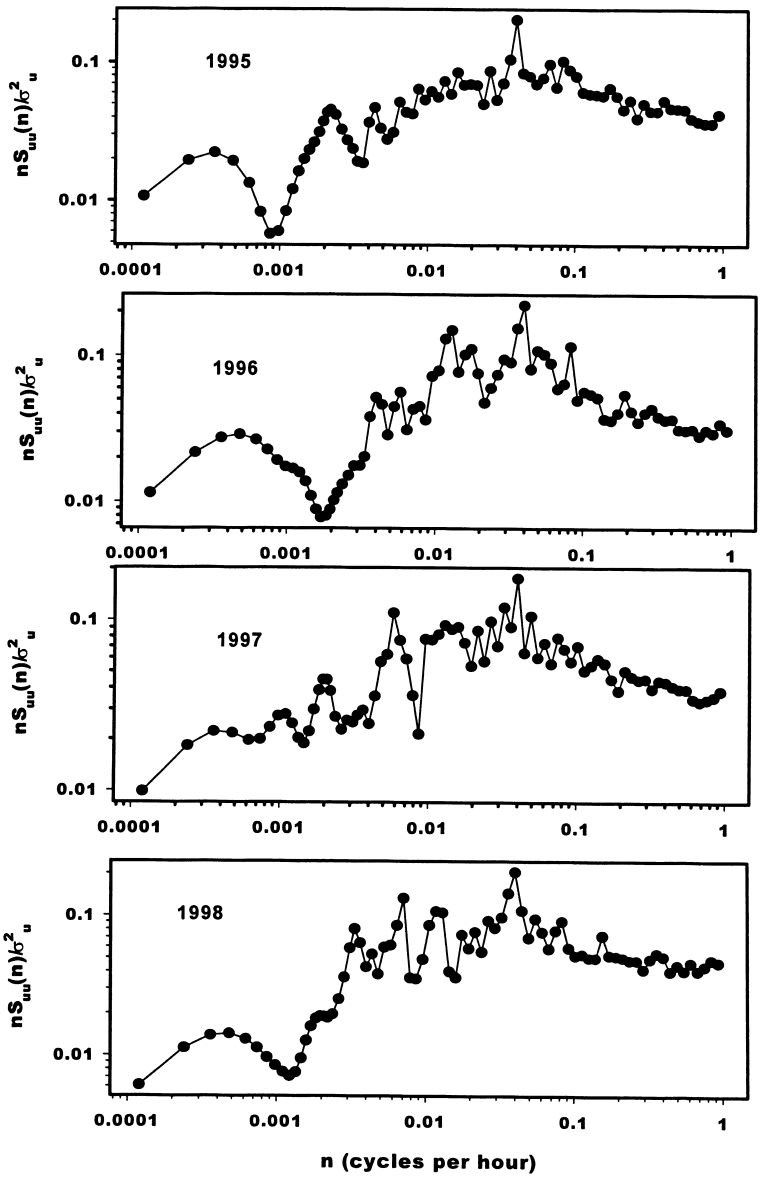

Fig. 5. Power spectrum for a year-long time series on wind speed. The spectral densities are multiplied by natural frequency, n, and are normalized by the variance of the time series. Spectra are presented for the years 1995 (a), 1996 (b), 1997 (c), and 1998 (d).

water vapor flux densities due to frontal passages or if pressure pumping is affecting the evolution of CO_2 from the soil (Kimball, 1983). Over periods ranging between months and hours, the spectral density of pressure decreases in a monotonic fashion with increasing frequency. The slopes of these spectra are near -1 and their values translate to slopes of -2 when plotted as a function of $S_p(n)$. These slopes match the measurements and theoretical arguments presented by Kimball and Lemon (1970), who reported that the pressure power spectrum falls with a $-\frac{6}{3}$ slope in the turbulence portion of the spectrum (frequencies ex-

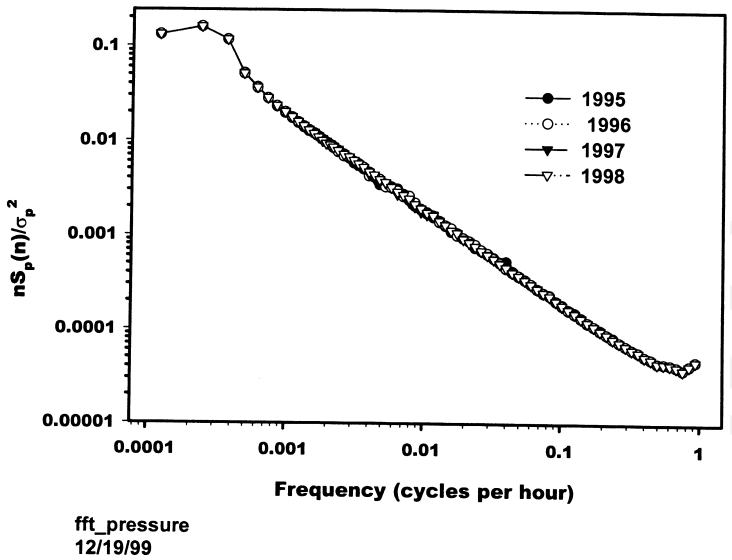

Fig. 6. Power spectrum for a year-long time series on air pressure. The spectral densities are multiplied by natural frequency, n, and are normalized by the variance of the time series. Spectra are presented for the years 1995 (a), 1996 (b), 1997 (c), and 1998 (d).

ceeding $1\,h^{-1}$). The data we present, however, suggest that the pressure power spectrum extends much further in time than was reported by Kimball and Lemon (1970).

3.3. Power spectra of mass and energy flux densities

Power spectra for flux densities of CO_2 (F_c) are presented in Fig. 7 for yearly periods between 1995 and 1998. The CO_2 flux density power spectrum exhibits several distinct features, as denoted by spectral peaks or gaps. All 4 years experience a low frequency peak ($n \sim 0.0004\,h^{-1}$) that corresponds with the spectral peaks of leaf area (Fig. 2), sunlight (Fig. 3) and air temperature (Fig. 4). Moving up in frequency, one encounters a distinct spectral gap. This feature varies considerably from year to year. In years 1995 through 1998, this gap occurred with periods of 20, 19, 28 and 27 days, respectively, which does not correspond with the spectral gap observed in Fig. 2 for leaf area index. The observance of a spectral gap with a 'month-long' periodicity occurs because no meaningful biological or meteorological factor has power at that period. The time scale of this spectral gap has implications on gap-filling procedures. These data suggest that a updating of gap-filling algorithms on a monthly basis is adequate to capture short and long time scale features of the flux record.

The next set of spectral peaks occurred with periodicities (frequencies) of 3.9 ($0.0107\,h^{-1}$), 4.8 ($0.00868\,h^{-1}$), 2.5 ($0.0166\,h^{-1}$) and 4.8 days during 1995 through 1998, respectively. A periodic sequence of clear and cloudy days following the passage of weather fronts will modulate canopy-scale CO_2 exchange (Baldocchi, 1997; Gu et al., 2000). We cannot discount the impact of changing wind direction on the spectral peaks with multi-day periods. Our site has an appreciable amount of loblolly pine in the northwest quadrant of the flux footprint, so any change of wind direction will alter the source/sink being viewed by the tower-based flux measurement system. Progressing further up the spectrum, we observe that all 4 years experienced pronounced spectral peaks with periodicities of 24 h ($0.0416\,h^{-1}$) and 12 h ($0.0833\,h^{-1}$). This observation was expected, as it is widely known that CO_2 exchange experiences a pronounced diurnal variation. Finally, noise is a feature of the power spectra at highest frequencies, or periods shorter than one-half of a day. We suspect noise occurs at high frequencies from natural run-to-run variability that is associated with eddy covariance measurements (Kaimal and Finnigan, 1994; Panofsky and Dutton, 1984).

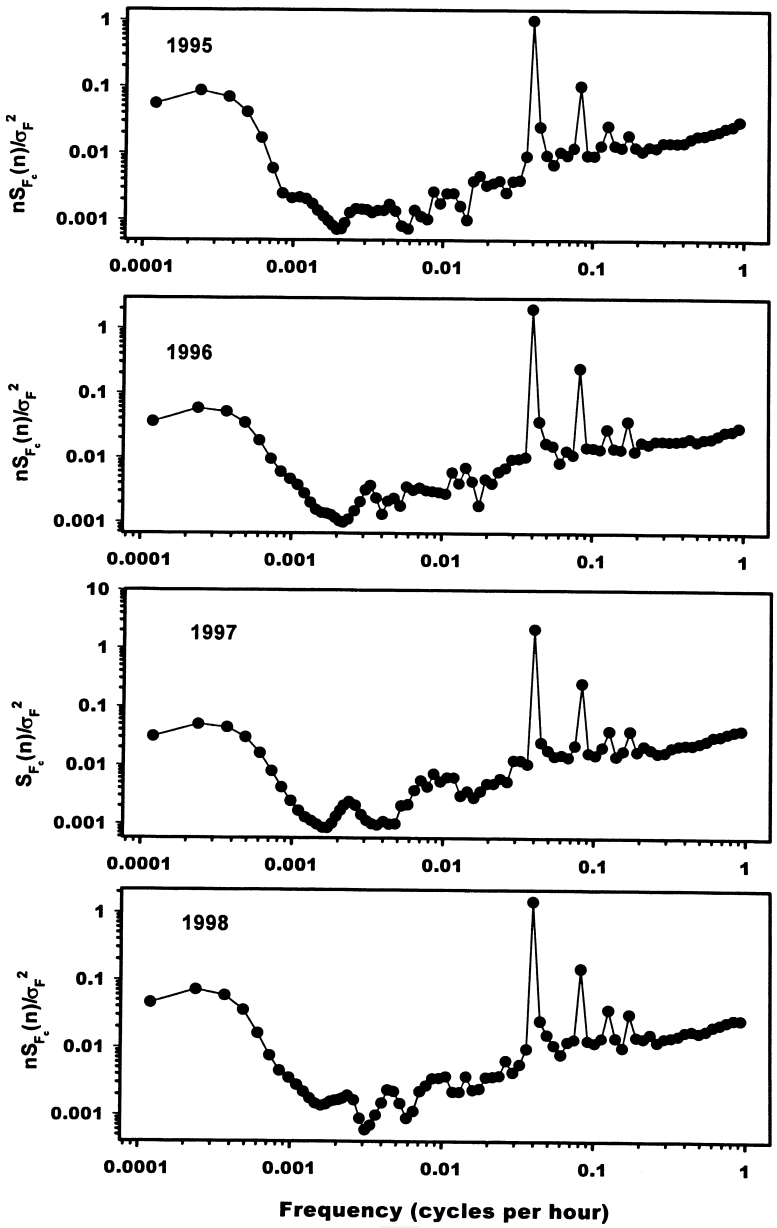

Fig. 7. Power spectrum for a year-long time series on CO_2 flux density (F_c). The spectral densities are multiplied by natural frequency, n, and are normalized by the variance of the time series. Spectra are presented for the years 1995 (a), 1996 (b), 1997 (c), and 1998 (d).

To quantify inter-annual variability of canopy CO_2 exchange we constructed a continuous 4-year time series consisting of daily sums and performed a Fourier transform upon those data. Fig. 8 shows that distinct spectral peaks occur at periods of 342 days (0.00292 per day), 120 days (0.00833 per day), 52 days (0.0192 per day), 17 days (0.0588 per day) and 3.7 days (0.222 per day). The longest and shortest periods correspond with times scale associated with the annual cycle and the passage of weather fronts.

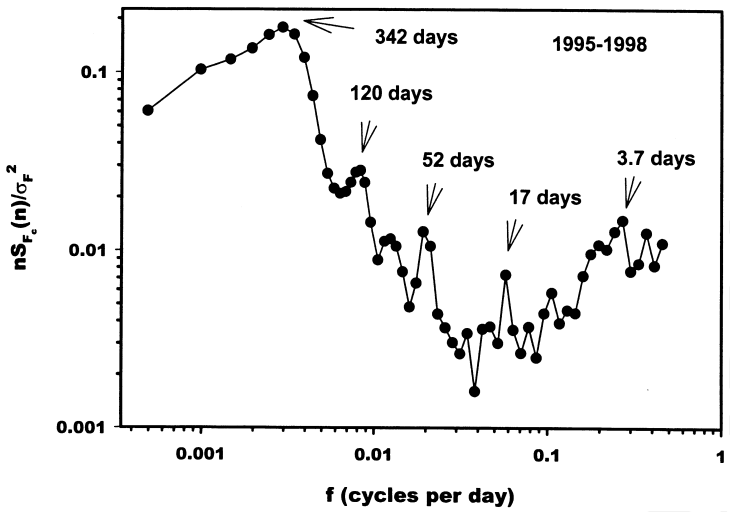

Fig. 8. Power spectrum for a continuous record of daily integrated fluxes of CO_2 between 1995 and 1998.

No spectral peak was observed at multi-year time scales, despite year-to-year differences in climate and growing season length. However, significant amounts of power are associated with periods of 2 through 4 years, as compared to higher frequency spectral peaks. An interesting feature of the multi-year spectrum is that we lose the semi-annual and quarterly spectral peaks (that were seen in the annual spectra) and gain spectral peaks with shorter periods (120 and 52 days), which do not correspond with any noted biological or meteorological periodicity.

Yearly scale power spectra for latent heat flux densities are presented in Fig. 9. If one overlays the power spectra for latent heat and CO_2 flux densities, one finds a similar spectral pattern, but one does not find perfect correspondence between spectral gaps and peaks. We discuss this issue below when we compute the co-spectrum between F_{wpl} and λE.

3.4. Co-spectra, coherence and phase angles

Fig. 10 shows the co-spectrum between F_c and Q_p, measured during 1997 — a representative year — as well as the coherence and phase angle spectra. The co-spectrum exhibits seasonal, daily and half-day spectral peaks and is flat on the hourly time scale (Fig. 10a). As with their respective power spectra, there is a pronounced co-spectral gap at the 'monthly' time scale ($0.001\,h^{-1}$).

The magnitude of coherence between F_c and Q_p (Fig. 10b) is low (less than 0.1) for the annual to seasonal co-spectral peak, as well as the monthly spectral gap. Highest coherence (>0.6) corresponds with a small weekly scale co-spectral peak and with the stronger daily and half-day scale peaks.

The phase angles between F_c and Q_p (Fig. 10c) are close to 180° on annual to semi-annual time scales ($n < 0.001$) and on daily time scales ($n > 0.1$). The 180° phase shift occurs between F_c and Q_p because the temporal course of sunlight is associated with the withdrawal of CO_2 from the atmosphere, a flux that possesses a negative sign. The most distinct phase shift between F_c and Q_p occurs at the monthly time scale, when the phase angle is about −120°. On week to daily time scales, the phase angle relation between F_c and Q_p swings back and forth between leading and lagging each other by 180°. Results from the other years are summarized in Table 3. For years 1995, 1996 and 1998, the phase angles between F_c and Q_p were close to 180° for annual, semi-annual and daily time scales, too.

A co-spectrum between F_c and air temperature (T_{air}) is presented in Fig. 11a. The greatest covariance occurs at the annual to seasonal and daily time scales. Furthermore, more covariance occurs under the low frequency peak portion of the co-spectrum for F_c and T_{air} than for F_c and Q_p (Fig. 10).

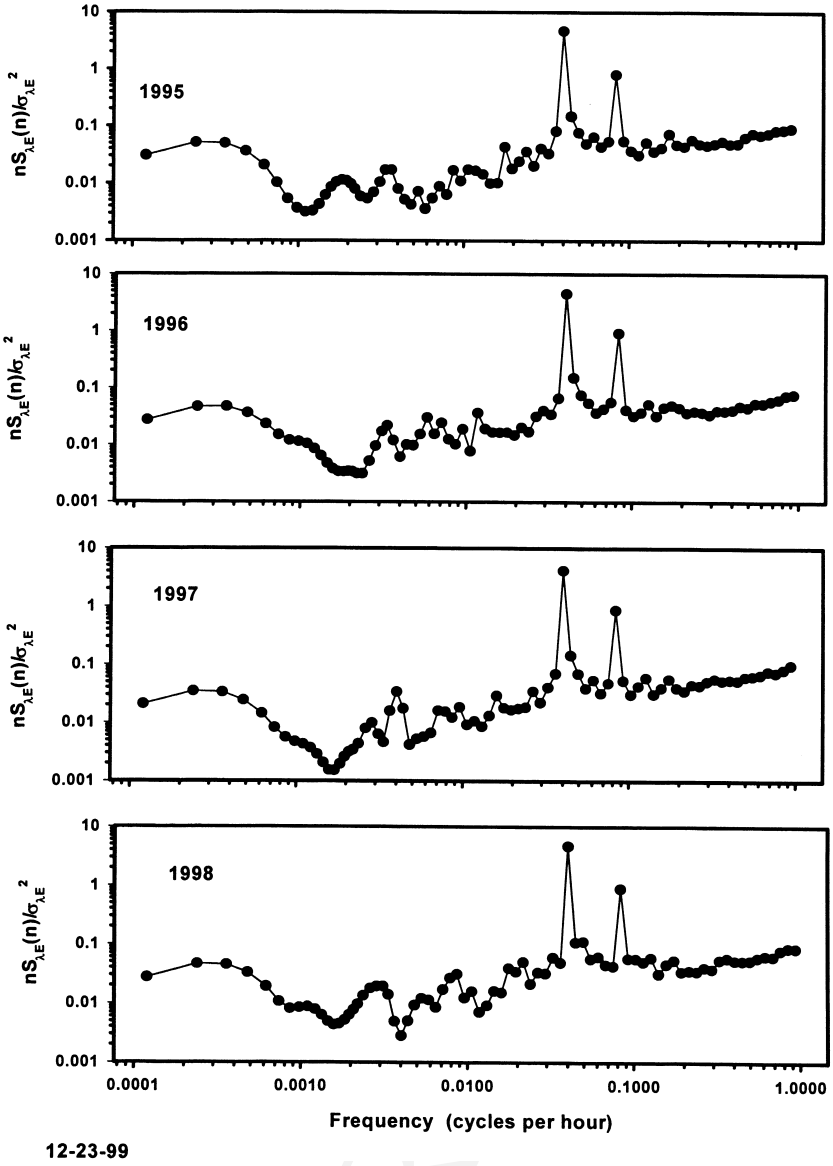

Fig. 9. Power spectrum for a year-long time series on latent heat flux density (λE). The spectral densities are multiplied by natural frequency, n, and are normalized by the variance of the time series. Spectra are presented for the years 1995 (a), 1996 (b), 1997 (c), and 1998 (d).

Like the photon flux and CO_2 flux density coherence spectra, the coherence between F_c and T_{air} is low at annual to seasonal periods (Fig. 11b). Except for the daily and half-day periods, coherence values are below 0.5 across the entire spectrum. These results suggest that one should not use only variations in sunlight to model CO_2 exchange of this forest, across a variety of time scales. We raise this point because many biogeochemical models estimate net and gross primary productivity on the basis of light use efficiency model of Kumar and Monteith (1981) (see Cramer et al., 1999).

The phase angle spectrum between F_c and T_{air} indicates that low frequency covariations between F_c and T_{air} experience a distinct 180° phase shift with one an-

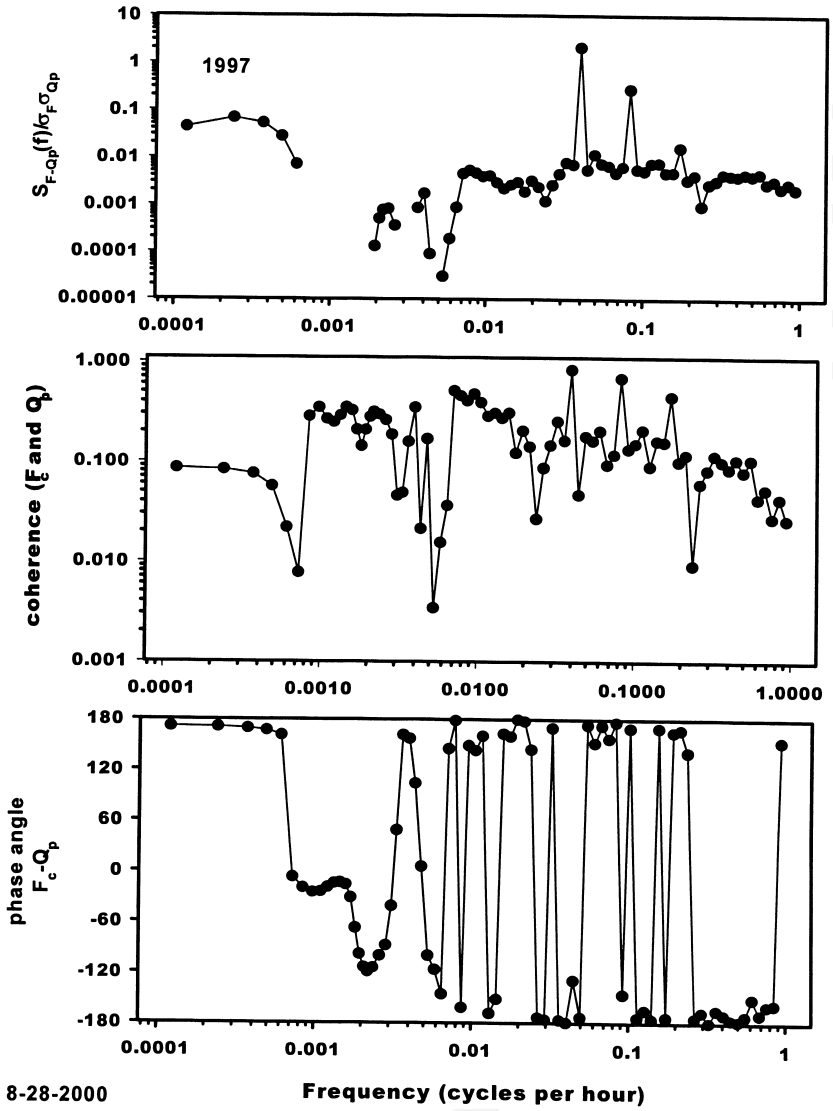

Fig. 10. (a) Co-spectrum for photosynthetically active radiation flux density (Q_p) and CO_2 flux density. The spectral densities are multiplied by natural frequency, n, and are normalized by the mean covariance of the two time series. The data were acquired during 1997. (b) Coherence spectrum for covariance between photosynthetically active radiation flux density (Q_p) and CO_2 flux density (F_c). The data are from 1997. (c) Phase angle spectrum for covariance between photosynthetically active radiation flux density (Q_p) and CO_2 flux density (F_c). The data are from 1997.

other (Fig. 11c). This observation is the consequence of an enhancement of carbon uptake with positive perturbations in air temperature on time scales of seasons to years. At daily time scales the phase angle between F_c and T_{air} is on the order of 132°. This lag can be explained by the strong dependence of canopy photosynthesis on available light (e.g. Ruimy et al., 1995) and the subsequent 2–3 h lag that typically occurs between the daily course of sunlight and air temperature.

On the basis of studying temporal changes in atmospheric CO_2, a group of scientists has recently inferred how CO_2 concentrations and temperature

Table 3
Phase angle at the daily spectral peak (degrees) for the relation between CO_2 flux density and air temperature or quantum flux density

	$F_c - T_{air}$	$F_c - Q_p$
The data are for frequencies associated with one cycle per day		
1995	129	−179
1996	131	−179
1997	131	−179
1998	131	178
The data are for frequencies associated with one cycle per 180 days		
1995	175	175
1996	176	175
1997	170	170
1998	175	174
The data are for frequencies associated with one cycle per 347 days		
1995	175	174
1996	176	174
1997	170	174
1998	175	174

change relative with one another (Randerson et al., 1999). Changes in CO_2 and temperature are in phase during the winter. Then, an ecosystem loses carbon as it respires and respiration is closely coupled to temperature. During growing season CO_2 and temperature are out-of-phase. The dominant processes governing carbon exchange, then, are assimilation, which is driven primarily by available light (Ruimy et al., 1995), and respiration, a temperature-dependent process. A phase shift occurs because seasonal changes in temperature lag those in available light.

We are able to investigate and quantify these interactions further with the aid of direct CO_2 flux density measurements. To do so, we divided the 1997 data set into four segments, one for each season. With regard to seasonal scale frequencies ($n < 0.002\,h^{-1}$) CO_2 exchange during the winter dormant period possessed the most distinct phase angle difference with Q_p, a difference of 50° (Fig. 12; Table 4). On the other hand, CO_2 exchange was perfectly in phase with air temperature during the winter (Fig. 13; Table 4). This result is consistent with the results of Randerson et al. (1999) and is expected because respiration, by dormant temperate forests, is correlated with changes in temperature (Raich and Schlesinger, 1992; Hanson et al., 1993). During the growing season and autumn, the phase angles between seasonal CO_2 exchange and Q_p and CO_2 exchange and air temperature were on the order of plus/minus 180°. During spring, the phase angles between F_c and Q_p and F_c and T_{air} were on the order of −163°, at low frequencies. These data indicate that one should exercise caution when forcing springtime CO_2 exchange with simple algorithms based on either light and/or temperature, as light and air temperature provide weaker forcing on CO_2 exchange during this period of rapid physiological and phenological change, compared to changes in physiological capacity.

The low frequency and seasonally varying contributions of temperature on CO_2 exchange implies that simple estimates of CO_2 exchange cannot be generated on the basis of algorithms that are forced by annual means. An equal temperature perturbation during the dormant and growing seasons will impose a different forcings on the net annual carbon flux (e.g. a year with a warm winter and cool summer will experience a different sum of net ecosystem–atmosphere CO_2 exchange from a year with a cool winter and warm summer, though both years experience the same annual mean temperature).

There is plentiful evidence showing that carbon assimilation scales with evaporation on hourly and daily time scales (Makela et al., 1996), but how well these two processes correspond over multiple time scales is unknown Fig. 14a shows the co-spectra between F_{wpl} and λE, Fig. 14b shows the coherence spectrum and

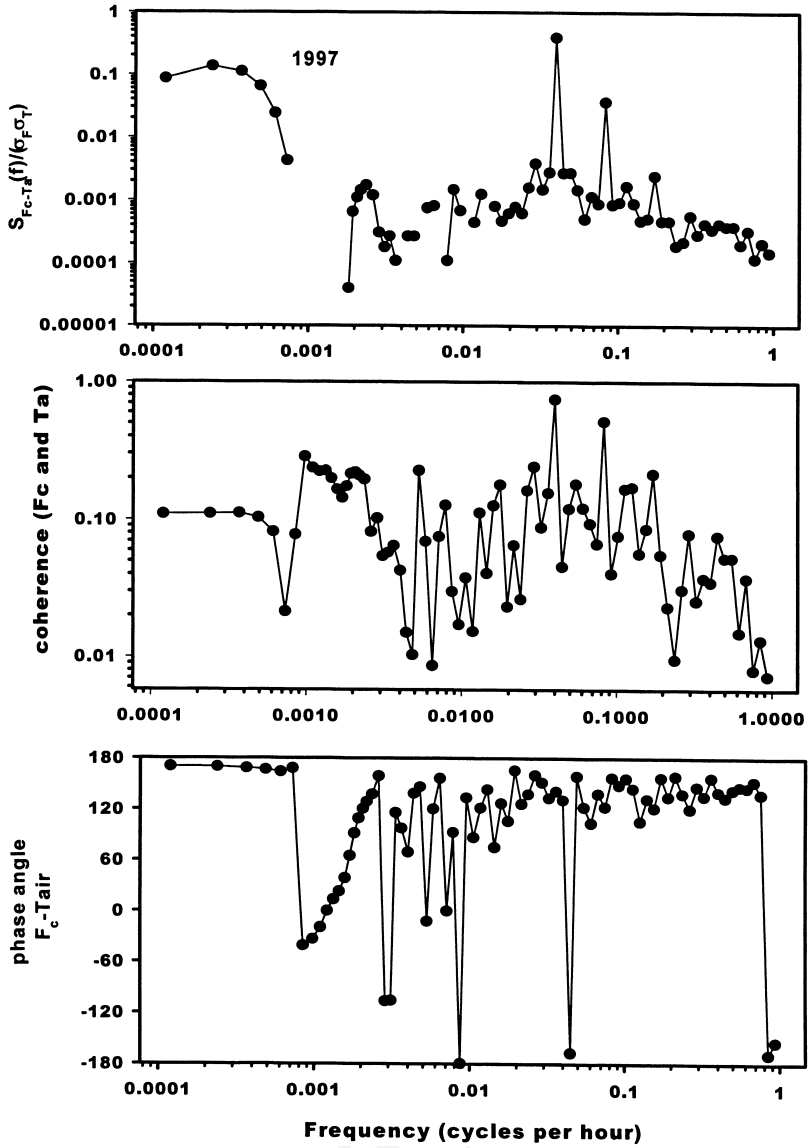

Fig. 11. (a) Co-spectrum for air temperature (T_a) and CO_2 flux density. The spectral densities are multiplied by natural frequency, n, and are normalized by the mean covariance of the two time series. The data are from 1997. (b) Coherence spectrum for covariance between air temperature (T_a) and CO_2 flux density (F_c). (c) Phase angle spectrum for covariance between air temperature (T_a) and CO_2 flux density (F_c).

Fig. 14c shows the associated phase angle spectra. Coherent and in-phase spectral peaks occur on annual, seasonal and daily time scales. In fact coherence values are greater for the F_c and λE, than those shown previously for sunlight and air temperate. At the monthly to weekly time scales (n between 0.001 and 0.003) the covariance between F_c and λE either diminishes or changes sign (and goes off scale). We also report that F_c lags λE by up to 90° in some instances and leads it by 60° in other instances. This behavior reflects the

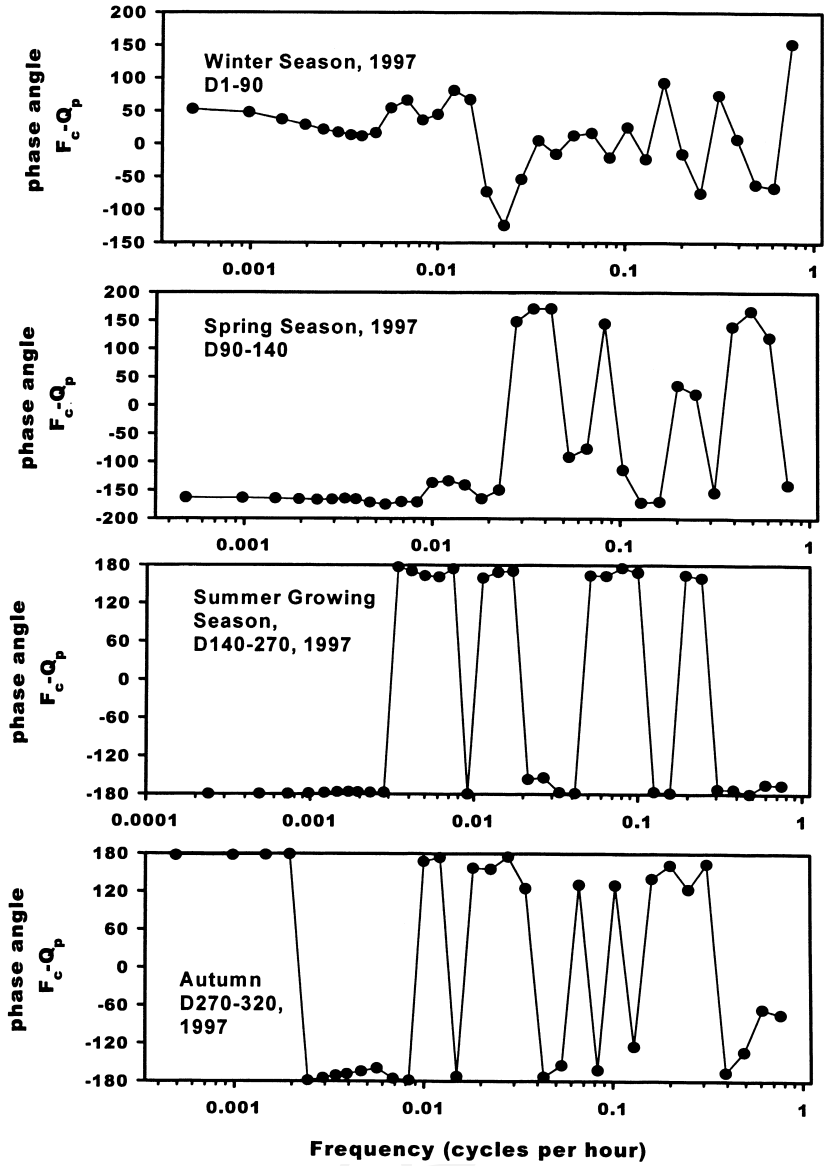

Fig. 12. Phase angle spectrum between photon flux density and CO_2 flux density on a seasonal basis during 1997: (a) winter, (b) spring, (c) summer, and (d) autumn.

impact of winter, when evaporation is low over the dormant forest (Wilson and Baldocchi, 2000) but the forest is respiring. Over a 12 h period, F_c often leads λE, as indicated by the spike. This distinct phase angle is as large as 40°. This feature reflects the impact of λE going to zero at night, while F_c changes sign as the ecosystem respires.

3.5. Modeling the spectrum of relevant time scales for canopy CO_2 exchange

At present biophysical, biogeochemical and biogeographic models are used to evaluate CO_2 exchange between the land and the atmosphere. The biophysical models operate at minute to hourly time scales (Sellers

et al., 1997; Baldocchi, 1997) biogeochemical models use daily to monthly time steps (Schimel et al., 1991, 1996) and the biogeographical models use monthly to annual time steps (Hurtt et al., 1998; Cramer et al., 1999). With the information presented in this paper we can address several questions that are relevant to modeling carbon and water fluxes over multiple time scales. First, how much information is needed to apply a biophysical model on longer times scales? And second, how well does a biophysical model replicate the spectral peaks and gaps we have identified in the experimental record? To address these questions, we employed the biophysical CANOAK model (Baldocchi, 1997). We attempt to model multiple scales of variance in CO_2 exchange by varying only input meteorology, leaf area index and photosynthetic capacity.

The model consists of coupled micrometeorological and physiological modules. The micrometeorological model computes leaf and soil energy exchange, turbulent diffusion, scalar concentration profiles and radiative transfer through the canopy at hourly time steps. Environmental variables, computed with the micrometeorological module, in turn, drive the physiological models that compute leaf photosynthesis, stomatal conductance, transpiration, and leaf, bole and soil/root respiration. The model is driven by a minimal number of external variables that were measured above the forest. Environmental inputs include incident photosynthetic photon flux density (Q_p), air and soil temperature, wind speed, relative humidity and CO_2 concentration. Temporal changes in leaf area and photosynthetic capacity are prescribed.

For a year with adequate soil moisture (1997), power spectra of CO_2 exchange that were generated using CANOAK model calculations and from field data overlap one another across time scales ranging from a year to half-day (Fig. 15a). The model does not reproduce the hourly noise that is associated with atmospheric flux measurements, however. This lacking may be attributed, in part, to our inability to measure nocturnal fluxes of CO_2 exchange well at this topographically undulating field site (see Baldocchi et al., 2000). Model calculations also overestimate spectral power of fluctuations that had a frequency of about $0.0005\,\text{cycles}\,\text{h}^{-1}$. Across the spectrum model calculations and measurements are nearly in-phase with one another with on yearly, seasonal, weekly and daily time scales (Fig. 15b).

Table 4
Phase angle at the seasonal spectral peak (degrees) for the relation between CO_2 flux density and air temperature or quantum flux density[a]

	$F_c - T_{air}$	$F_c - Q_p$
Winter dormant (D1-90)	0	52
Spring (D90-140)	−162	−163
Growing season (D140-270)	−179	−179
Autumn (270-320)	177	177

[a] The data are divided according to season. The data are from 1997.

During the year with a pronounced summer drought (1995), the model (which did not consider the role of soil water deficits on carbon assimilation and respiration) replicates time scales of variance in CO_2 exchange measurement record that had periods ranging from a week to half of a day (Fig. 16a). In contrast, model calculation fails to replicate the spectral peak that has a periodicity of about 10 days ($n \sim 0.004\,\text{h}^{-1}$). The model also underestimates the power associated with seasonal to annual time scales ($n < 0.0004\,\text{h}^{-1}$), although measurements and calculations are in phase at this time scale.

Another use of the information presented in this paper is to provide guidance on temporal resolution and seasonal dynamics to biophysical and biogeochemical cycling models that predict ecosystem-scale carbon dioxide exchange. How much variance do models, that use relatively crude time steps, miss? With regards of using biogeochemical and biogeographical models that have long time steps, we quantified the impact of spectral filtering by model class by computing the proportional variance (area) under the spectral curve for the daily, semi-annual and annual peaks of the power spectrum for CO_2 flux density. Twenty-one percent of the variance of CO_2 exchange over the course of a year is associated with the annual cycle, 43% of the variance is associated with the diurnal cycle and 9% is associated with the semi-annual time scale.

Non-linear forcings by environmental variables are ubiquitous with regard to the operation and performance of ecosystems (Rastetter et al., 1992; Leuning et al., 1995). One criticism levied at models that use daily and monthly time step models is that they ignore non-linear forcings that occur on shorter time scales. The expected value of a non-linear and co-varying function is proportional to the function evaluated at

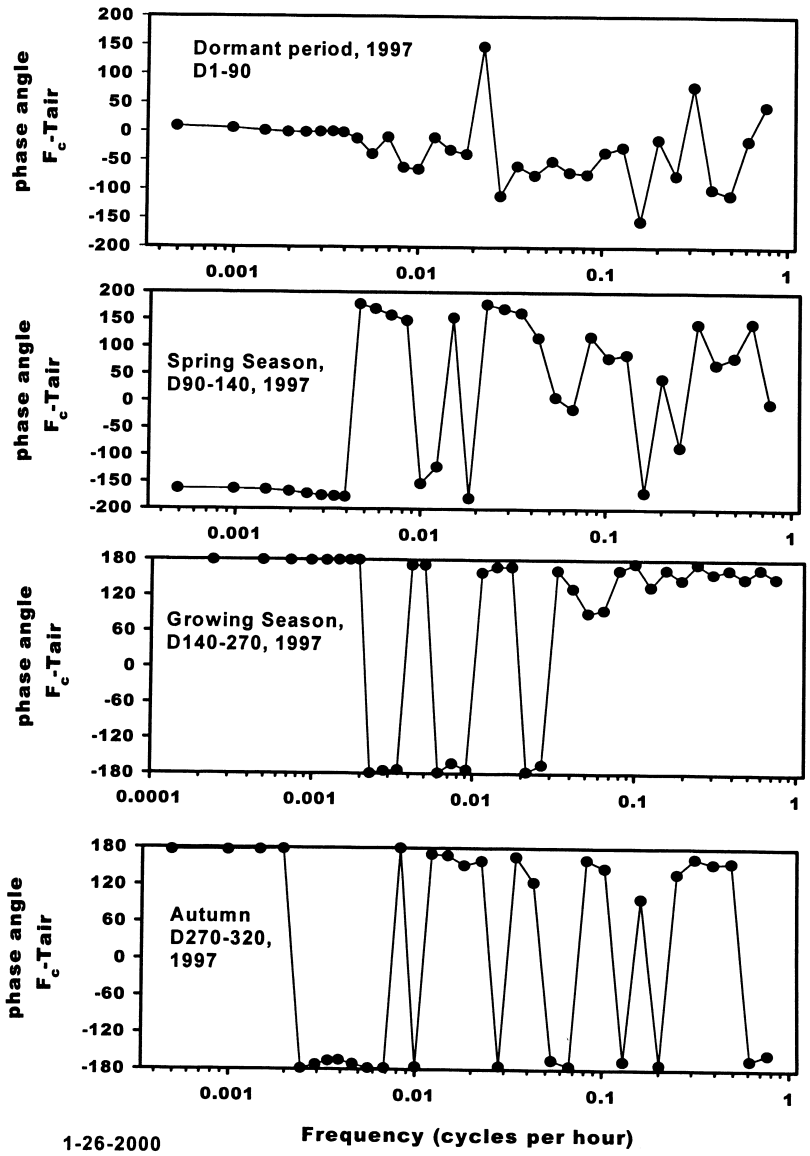

Fig. 13. Phase angle spectrum between air temperature and CO_2 flux density on a seasonal basis during 1997: (a) winter, (b) spring, (c) summer, and (d) autumn.

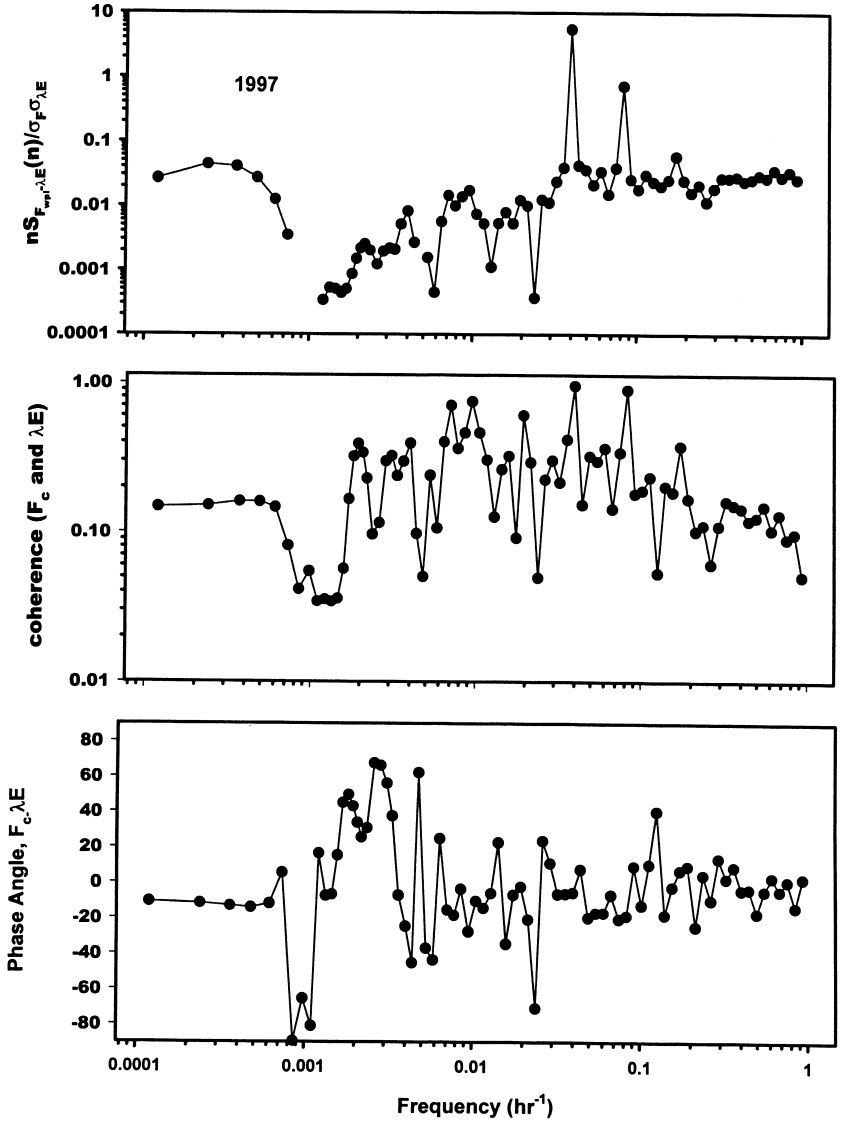

Fig. 14. (a) Co-spectrum for latent heat flux density (λE) and CO_2 flux density. The spectral densities are multiplied by natural frequency, n, and are normalized by the mean covariance of the two time series. Spectra are presented for 1997. (b) Coherence spectrum for covariance between latent heat flux density (λE) and CO_2 flux density (F_c). (c) Phase angle spectrum for covariance between latent heat flux density (λE) and CO_2 flux density (F_c).

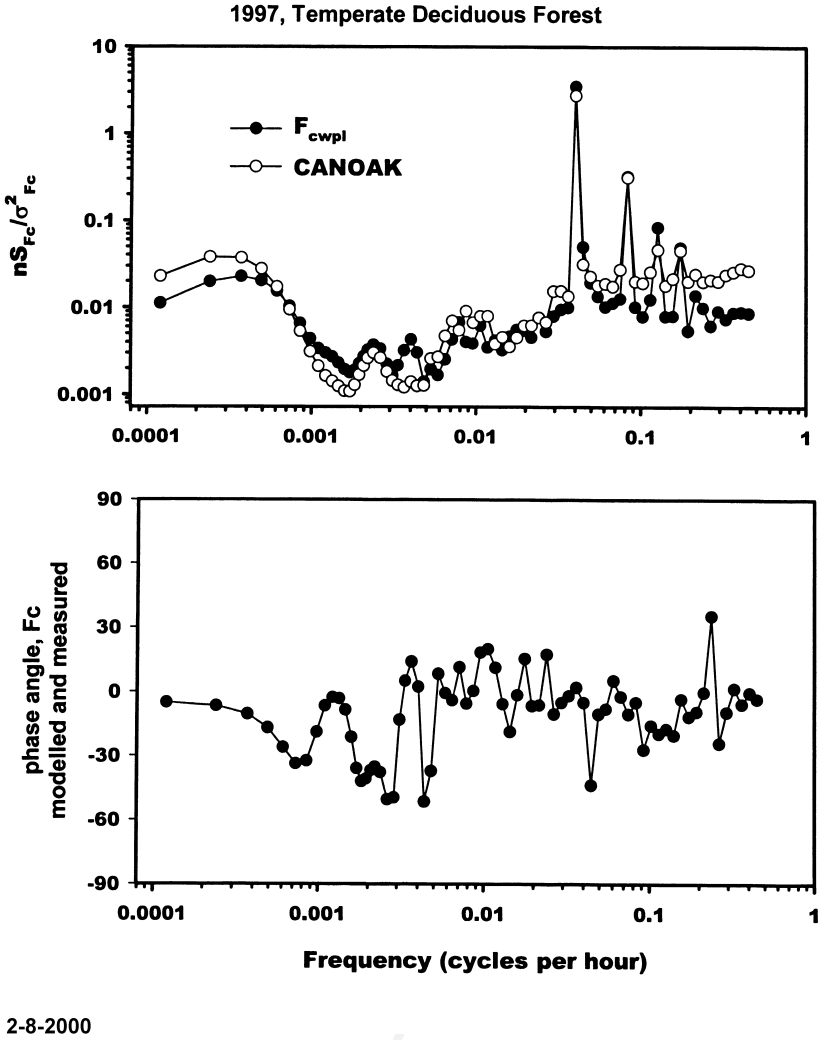

Fig. 15. (a) Power spectra of CO_2 flux densities that were measured with the eddy covariance method and computed with the CANOAK model. Data are presented for 1997 (a wet year). (b)The phase angle between measured and calculated values of canopy CO_2 exchange.

the means plus a term that is a function of the variance or covariance, respectively:

$$E[x \cdot x] \sim \overline{x \cdot x} + \overline{x'x'} \quad (3)$$

$$E[x \cdot y] \sim \overline{x \cdot y} + \overline{x'y'} \quad (4)$$

where over bars denote averaging and primes denote fluctuations from the mean; these relations can be derived using either Taylor's expansion series or Reynolds' averaging rules. If there is significant covariance at a finer time scale, then information is be lost by ignoring variance and covariance terms. The results in this paper show significant variance and covariance at daily times scales. This is information that coarse resolution models will miss using monthly time steps.

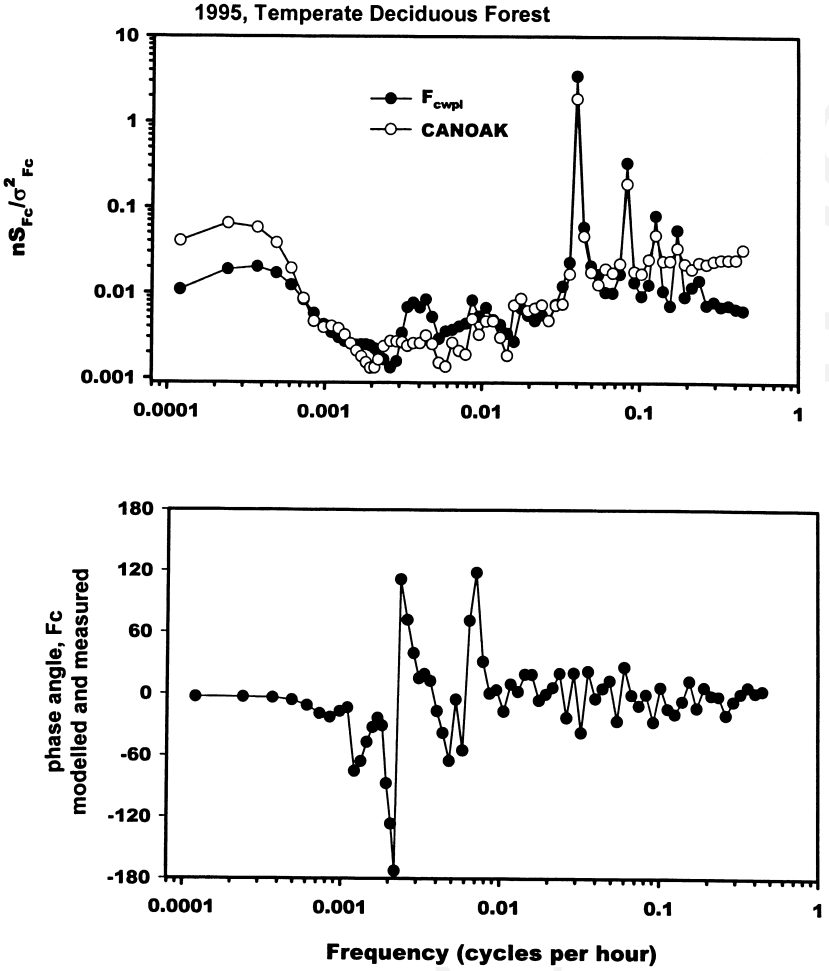

Fig. 16. (a) Power spectra of CO_2 flux densities that were measured with the eddy covariance method and computed with the CANOAK model. Data are presented for 1995 (a dry year). (b) The phase angle spectrum between measured and calculated values of canopy CO_2 exchange.

4. Conclusions

Fourier analysis of long time series of carbon dioxide and water vapor exchange provide information on time scales of variance and covariance in the records of CO_2 and water vapor exchange that are not readily detectable by examining their time series. We detected significant variance at times scales of a day and season, as expected and, we saw significant variance at the time scale of weeks and a pronounced spectral gap on the time scale of a month, which is rarely quantified.

Of particular note is the ability of Fourier analysis to inspect if model calculations of CO_2 and water vapor exchange are capturing the various spectral peaks and gaps that are identified in the experimental record. By varying meteorology, leaf area index and photosynthetic capacity we are able to replicate most of the spectral gaps and peaks that are associated with CO_2 exchange, when soil moisture is ample. By not accounting for the effects of summer droughts on computing CO_2 flux densities we are unable to account for a spectral peak that has a periodicity of 10 days.

In the future, we intend to apply Fourier analysis to the time series of flux measurements at other field sites across the FLUXNET network (see Running et al., 1999). We intend to examine spectral patterns at sites with contrasting climates and different seasonality, such as boreal and tropical forests, savanna woodlands and crops.

Spectral information on mass and energy exchange has potential for guiding gap-filling procedures (Falge et al., 2000). At present some investigators are constructing binned averaged diurnal patterns, over a specified interval, to estimate missing CO_2 fluxes (Moncrieff et al., 1996; Jarvis et al., 1997; Baldocchi, 1997). If the averaging period is too short then the constructed means possess relatively large sampling errors (Moncrieff et al., 1996). If the averaging period is too long, then one introduces low frequency noise on the average by incorporating seasonal trends. The prominent spectral gap at monthly time scales indicates that monthly re-evaluation of gap-filling algorithms is adequate.

In closing, we acknowledge that wavelet analysis may be another worthwhile tool with which to examine long records of mass and energy exchange data (Gabriel Katul, personal communication). Wavelets produce spectra that are local in time, and hence have the potential to dissect the impact of such phenomena as regional scale droughts or prolonged cloudy periods across a net work of sites. Another alternative is Lomb's periodogram method (Press et al., 1992), as it can be applied to the data sets with natural gaps.

Acknowledgements

This work is supported by the US Department of Energy's Terrestrial Carbon Program, NASA's GEWEX/GCIP program, NASA's EOS Validation Project and the University of California's Agricultural Experiment Station. This work contributes to the AmeriFlux and FLUXNET programs.

We thank Mark Hall, Mark Brewer, David Auble and Dr. Detlef Matt from NOAA/ATDD for their assistance in the acquisition of the field data. We thank Dr. Paul Hanson of Oak Ridge National Laboratory for supplying leaf area index measurements. We thank Dr. Roland Stull for advice on some recent long-term wind spectra measurements and Drs. Lianhong Gu and James Randerson for an internal reviews of the manuscript.

References

Amiro, B.D., 1998. Footprint climatologies for evapotranspiration in a boreal catchment. Agric. For. Meteorol. 90, 195–201.

Anderson, D.E., Verma, S.B., Clement, R.E., Baldocchi, D.D., Matt, D.R., 1986. Turbulence spectra of CO_2, water vapor, temperature and velocity over a deciduous forest. Agric. For. Meteorol. 38, 81–99.

Auble, D.L., Meyers, T.P., 1992. An open path, fast response infrared absorption gas analyzer for H_2O and CO_2. Boundary Layer Meteorol. 59, 243–256.

Baldocchi, D.D., 1997. Measuring and modeling carbon dioxide and water vapor exchange over a temperate broad-leaved forest during the 1995 summer drought. Plant Cell Environ. 20, 1108–1122.

Baldocchi, D.D., Wilson, K.B., 2000. Modeling CO_2 and water vapor exchange of a temperate broad-leaved forest across hourly to decadal time scales. Ecol. Model., submitted for publication.

Baldocchi, D.D., Finnigan, J.J., Wilson, K.W., Paw U, K.T., Falge, E., 2000. On measuring net ecosystem carbon exchange in complex terrain over tall vegetation. Boundary Layer Meteorol. 96, 257–291.

Black, T.A., den Hartog, G., Neumann, H., Blanken, P., Yang, P., Nesic, Z., Chen, S., Russel, C., Voroney, P., Staebler, R., 1996. Annual cycles of CO_2 and water vapor fluxes above and within a Boreal aspen stand. Global Change Biol. 2, 219–230.

Bracewell, R.N., 1990. Numerical transforms. Science 248, 697–704.

Braswell, B.H., Schimel, D.S., Linder, E., Moore III, B., 1997. The response of global terrestrial ecosystems to interannual temperature variability. Science 278, 870–872.

Brubaker, K.L., Entekhabi, D., 1996. Analysis of feedback mechanisms in land–atmosphere interaction. Water Resour. Res. 32, 1343–1357.

Carter, G.C., Ferrier, J.F., 1979. A coherence and cross spectral estimation program. In: Digital Processing Committee (Eds.), Programs for Digital Signal Processing. IEEE Press, New York.

Clements, W.E., Wilkening, M.H., 1974. Atmospheric pressure effects on 222Rn transport across the earth–air interface. J. Geophys. Res. 79, 5025–5029.

Cramer, W., Kicklighter, D.W., Bondeau, A., et al., 1999. Comparing global models of terrestrial net primary productivity: overview and key results. Global Change Biol. 5, 1–15.

Falge, E., Baldocchi, D., Valentini, R., Hollinger, D., Olson, R., Anthoni, P., Aubinet, M., Clement, R., Granier, A., Grünwald, T., Katul, G., Kowalsky, A., Meyers, T., Moors, E.J., Munger, B., Pilegaard, K., Rannik, U., Rebmann, C., Verma, S., 2000. Gap filling strategies for defensible annual sums of net ecosystem exchange. Agric. For. Meteorol., submitted for publication.

Fennessy, M.J., Shukla, J., 1999. Impact of initial soil wetness on seasonal atmospheric prediction. J. Climate 12, 3167–3180.

Goulden, M.L., Daube, B.C., Fan, S.M., Sutton, D.J., Bazzaz, A., Munger, J.W., Wofsy, S.C., J. Geophys. Res. Atmos. 102 (24) (1997) 28987–28996.

Greco, S., Baldocchi, D.D., 1996. Seasonal variations of CO_2 and water vapour exchange rates over a temperate deciduous forest. Global Change Biol. 2, 183–198.

Gu, L., Fuentes, J.D., Shugart, H.H., Staebler, R.M., Black, T.A., 2000. Responses of net ecosystem exchanges of carbon dioxide to changes in cloudiness: results form two North American deciduous forests. J. Geophys. Res. 104, 31421–31434.

Hamming, R.W., 1989. Digital Filters. Dover, New York, 284 pp.

Hanson, P.J., Wullschleger, S.D., Bohlman, S.A., Todd, D.E., 1993. Seasonal and topographic patterns of forest floor CO_2 efflux from an upland oak forest. Tree Physiol. 13, 1–15.

Heggem, T., Lende, R., Lovseth, J., 1998. Analysis of long time series of coastal wind. J. Atmos. Sci. 55, 2907–2917.

Heusser, L., Heusser, C., Kleczkowski, A., Crowhurst, S., 1999. A 50,000-yr pollen record from Chile of South American millennial-scale climate instability during the last glaciation. Quart. Res. 52, 154–158.

Hollinger, D.Y., Kelliher, F.M., Byers, J.N., Hunt, J.E., McSeveny, T.M., Weir, P.L., 1994. Carbon dioxide exchange between an undisturbed old-growth temperate forest and the atmosphere. Ecology 75, 134–150.

Hurtt, G.C., Moorcroft, P.R., Pacala, S.W., Levin, S.A., 1998. Terrestrial models and global change: challenges for the future. Global Change Biol. 4, 581–590.

Hutchison, B.A., Baldocchi, D.D., 1989. Forest meteorology. In: Johnson, D.W., Van Hook, R.I. (Eds.), Analysis of Biogeochemical Cycling Processes in Walker Branch Watershed. Springer, Berlin, pp. 21–95.

Jarvis, P.G., 1995. Scaling processes and problems. Plant Cell Environ. 18, 1079–1089.

Jarvis, P.G., Miranda, H.S., Muetzelfeldt, R.I., 1985. Modeling canopy exchanges of water vapour and carbon dioxide in coniferous forest plantations. In: Hutchison, B.A., Hicks, B.B. (Eds.), The Forest–Atmosphere Interaction. Reidel, Dordrecht, pp. 521–542.

Jarvis, P.G., Massheder, J., Hale, S., Moncrieff, J., Rayment, M., Scott, S., 1997. Seasonal variation of carbon dioxide, water vapor and energy exchanges of a boreal black spruce forest. J. Geophys. Res. 102, 28953–28967.

Jones, H.G., 1983. Plants and Microclimate. Cambridge University Press, Cambridge.

Kaimal, J.C., Finnigan, J.J., 1994. Atmospheric Boundary Layer Flows: their Structure and Measurement. Oxford University Press, Oxford, 289 pp.

Kaimal, J.C., Wyngaard, J.C., Izumi, Y., Cote, O.R., 1972. Spectral characteristics of surface layer turbulence. Quart. J. R. Meteorol. Soc. 98, 563–589.

Keeling, C.D., Chin, J.F.S., Whorf, T.P., 1996. Increased activity of northern vegetation inferred from atmospheric CO_2 measurements. Nature 382, 146–149.

Kimball, B.A., 1983. Canopy gas exchange: gas exchange with soil. In: Limitations to Efficient Water Use in Crop Production. Agronomy Society of America, pp. 215–226.

Kimball, B.A., Lemon, E.R., 1970. Spectra of air pressure fluctuations at the soil surface. J. Geophys. Res. 75, 6771–6777.

Kumar, M., Monteith, J.L., 1981. Remote sensing of crop growth. In: Smith, H. (Ed.), Plants and the Daylight Spectrum. Academic Press, San Diego, CA, pp. 133–144.

Leuning, R., Kelliher, F.M., dePury, D., Schulze, E.D., 1995. Leaf nitrogen, photosynthesis, conductance and transpiration: scaling from leaves to canopies. Plant Cell Environ. 18, 1183–1200.

Lieth, H., 1975. Modeling the primary productivity of the world. In: Lieth, H., Whittaker, R.H. (Eds.), Primary Productivity of the Biosphere. Ecological Studies, Vol. 14. Springer, Berlin, pp. 237–264.

Makela, A., Berninger, F., Hari, P., 1996. Optimal control of gas exchange during drought: theoretical analysis. Ann. Bot. 77, 461–467.

Moncrieff, J.B., Mahli, Y., Leuning, R., 1996. The propagation of errors in long term measurements of land atmosphere fluxes of carbon and water. Global Change Biol. 2, 231–240.

Myneni, R.B., Keeling, C.D., Tucker, C.J., Asrar, G., Nemani, R.R., 1997. Increased plant growth in the northern high latitudes from 1981 to 1991. Nature 386, 698–702.

Panofsky, H.A., Dutton, J.A., 1984. Atmospheric Turbulence: Models and Methods for Engineering Applications. Wiley, New York.

Paw U, K.T., Baldocchi, D.D., Meyers, T.P., Wilson, K.B., 2000. Correction of eddy covariance measurements incorporating both advective effects and density fluxes. Boundary Layer Meteorol., in press.

Pearcy, R.W., 1990. Sunflecks and photosynthesis in plant canopies. Ann. Rev. Plant Physiol. Mol. Biol. 41, 421–453.

Pielke, R.A., Avissar, R., Raupach, M., Dolman, A.J., Zeng, X.B., Denning, A.S., 1998. Interactions between the atmosphere and terrestrial ecosystems: influence on weather and climate. Global Change Biol. 4, 461–475.

Press, W.H., Teukolsky, S.A., Vetteerling, W.T., Flannery, B.P., 1992. Numerical Recipes in C: The Art of Scientific Computing. Cambridge University Press, Cambridge, 994 pp.

Raich, J.W., Schlesinger, W.H., 1992. The global carbon dioxide flux in soil respiration and its relationship to vegetation and climate. Tellus B 44, 81–99.

Randerson, J.T., Field, C.B., Fung, I.Y., Tans, P.P., 1999. Increases in early season ecosystem uptake explain recent changes in the seasonal cycle of atmospheric CO_2 at high northern latitudes. Geophys. Res. Lett. 26, 2765–2768.

Rastetter, E.B., King, A.W., Cosby, B.J., Hornberger, G.M., O'Neill, R.V., Hobbie, J.E., 1992. Aggregating fine-scale ecological knowledge to model coarser-scale attributes of ecosystems. Ecol. Appl. 2, 55–70.

Ridgewell, A.J., Watson, A.J., Raymo, M.E., 1999. Is the spectral signature of the 100-yr glacial cycle consistent with a Milankovitch origin? Paleoceanography 4, 437–440.

Ruimy, A., Jarvis, P.G., Baldocchi, D.D., Saugier, B., 1995. CO_2 fluxes over plant canopies and solar radiation: a literature review. Adv. Ecol. Res. 26, 1–68.

Running, S.W., Baldocchi, D.D., Turner, D., Gower, S.T., Bakwin, P., Hibbard, K., 1999. A global terrestrial monitoring network, scaling tower fluxes with ecosystem modeling and EOS satellite data. Remote Sensing Environ. 70, 108–127.

Schimel, D.S., Kittell, T.G., Parton, W.J., 1991. Terrestrial biogeochemical cycles: global interactions with the atmosphere and hydrology. Tellus 43AB, 188–203.

Schimel, D.S., Braswell, B.H., McKeown, R., Ojima, D.S., Parton, W.J., Pulliam, W., 1996. Climate and nitrogen controls on the geography and timescales of terrestrial biogeochemical cycling. Global Biogeochem. Cycles 10, 677–692.

Schwartz, M.D., 1996. Examining the spring discontinuity in daily temperature ranges. J. Climate 9, 803–808.

Sellers, P.J., Dickinson, R.E., Randall, D.A., Betts, A.K., Hall, F.G., Berry, J.A., Collatz, G.J., Denning, A.S., Mooney, H.A., Nobre, C.A., Sato, N., Field, C.B., Henderson-Sellers, A., 1997. Modeling the exchanges of energy, water, and carbon between continents and the atmosphere. Science 275, 502–509.

Su, H.B., Paw U, K.T., Shaw, R.H., 1996. Development of a coupled leaf and canopy model for the simulation of plant–atmosphere interaction. J. Appl. Meteorol. 35, 733–748.

Turchin, P., Taylor, A.D., 1992. Complex dynamics in ecological time series. Ecology 73, 289–305.

Valentini, R., de Angelis, P., Matteucci, G., Monaco, R., Dore, S., Scarascia-Mugnozza, G.E., 1996. Seasonal net carbon dioxide exchange of a beech forest with the atmosphere. Global Change Biol. 2, 199–208.

Valentini, R., Matteucci, G., Dolman, A.J., et al., 2000. Respiration as the main determinant of carbon balance in European forests. Nature 404, 861–864.

Van der Hoven, I., 1957. Power spectrum of horizontal wind speed in the frequency range from 0.0007 to 900 cycles per hour. J. Meteorol. 14, 160.

Verma, S.B., Baldocchi, D.D., Anderson, D.E., Matt, D.R., Clement, R.E., 1986. Eddy fluxes of CO_2, water vapor and sensible heat over a deciduous forest. Boundary Layer Meteorol. 36, 71–91.

Webb, E.K., Pearman, G., Leuning, R., 1980. Correction of flux measurements for density effects due to heat and water vapor transfer. Quart. J. R. Meteorol. Soc. 106, 85–100.

Wikle, C.K., Milliff, R.F., Large, W.G., 1999. Surface wind variability on spatial scales from 1 to 1000 km observed during TOGA COARE. J. Atmos. Sci. 56, 2222–2231.

Wilson, K.B., Baldocchi, D.D., 2000. Seasonal and interannual variability of energy fluxes over a broad-leaved temperate deciduous forest. Agric. For. Meteorol. 100, 1–18.

Wilson, K.B., Baldocchi, D.D., Hanson, P.J., 2000. Spatial and seasonal variability of photosynthesis parameters and their relationship to leaf nitrogen in a deciduous forest. Tree Physiol. 20, 787–797.

Zeng, X., Pielke, R.A., Eykholt, R., 1990. Chaos in daisy world. Tellus B 42, 309–318.